

# In Vivo Evaluation and Small-Animal PET/CT of a Prostate Cancer Mouse Model Using $^{64}\text{Cu}$ Bombesin Analogs: Side-by-Side Comparison of the CB-TE2A and DOTA Chelation Systems

Jered C. Garrison<sup>1,2</sup>, Tammy L. Rold<sup>1,2</sup>, Gary L. Sieckman<sup>1,2</sup>, Said Daibes Figueroa<sup>1,3</sup>, Wynn A. Volkert<sup>1,3</sup>, Silvia S. Jurisson<sup>4</sup>, and Timothy J. Hoffman<sup>1,2,4</sup>

<sup>1</sup>Harry S. Truman Memorial VA Hospital, Columbia, Missouri; <sup>2</sup>Department of Internal Medicine, University of Missouri–Columbia School of Medicine, Columbia, Missouri; <sup>3</sup>Department of Radiology, University of Missouri–Columbia School of Medicine, Columbia, Missouri; and <sup>4</sup>Department of Chemistry, University of Missouri–Columbia, Columbia, Missouri

The BB2 receptor subtype, of the bombesin family of receptors, has been shown to be highly overexpressed in a variety of human tumors, including prostate cancer. Bombesin (BBN), a 14-amino acid peptide, has been shown to target the BB2 receptor with high affinity.  $^{64}\text{Cu}$  (half-life = 12.7 h,  $\beta^+$ : 18%,  $E_{\beta^+ \text{max}}$  = 653 keV;  $\beta^-$ : 37%,  $E_{\beta^- \text{max}}$  = 578 keV) is a radioisotope that has clinical potential for application in both diagnostic imaging and radionuclide therapy. Recently, new chelation systems such as 1,4,8,11-tetraazabicyclo[6.6.2]hexadecane-4,11-diacetic acid (CB-TE2A) have been reported to significantly stabilize the  $^{64}\text{Cu}$  radiometal in vivo. The increased stability of the  $^{64}\text{Cu}$ -CB-TE2A chelate complex has been shown to significantly reduce nontarget retention compared with tetraazamacrocycles such as 1,4,7,10-tetraazacyclododecane-*N,N',N'',N'''*-tetraacetic acid (DOTA). The aim of this study was to determine whether the CB-TE2A chelation system could significantly improve the in vivo stability of  $^{64}\text{Cu}$  bombesin analogs. The study directly compares  $^{64}\text{Cu}$  bombesin analogs using the CB-TE2A and DOTA chelation systems in a prostate cancer xenograft SCID (severely compromised immunodeficient) mouse model. **Methods:** The CB-TE2A-8-AOC-BBN(7–14) $\text{NH}_2$  and DOTA-8-AOC-BBN(7–14) $\text{NH}_2$  conjugates were synthesized and radiolabeled with  $^{64}\text{Cu}$ . The receptor-binding affinity and internalization profile of each metallated conjugate was evaluated using PC-3 cells. Pharmacokinetic and small-animal PET/CT studies were performed using female SCID mice bearing PC-3 xenografts. **Results:** In vivo BB2 receptor targeting was confirmed by tumor uptake values of  $6.95 \pm 2.27$  and  $4.95 \pm 0.91$  %ID/g (percentage injected dose per gram) at the 15-min time point for the  $^{64}\text{Cu}$ -CB-TE2A and  $^{64}\text{Cu}$ -DOTA radioconjugates, respectively. At the 24-h time point, liver uptake was substantially reduced for the  $^{64}\text{Cu}$ -CB-TE2A radioconjugate ( $0.21 \pm 0.06$  %ID/g) compared with the  $^{64}\text{Cu}$ -DOTA radioconjugate ( $7.80 \pm 1.51$  %ID/g). The  $^{64}\text{Cu}$ -CB-TE2A-8-AOC-BBN(7–14) $\text{NH}_2$  radioconjugate demonstrated sig-

nificant clearance,  $98.60 \pm 0.28$  %ID, from the mouse at 24 h after injection. In contrast, only  $67.84 \pm 5.43$  %ID of the  $^{64}\text{Cu}$  activity was excreted using the  $^{64}\text{Cu}$ -DOTA-8-AOC-BBN(7–14) $\text{NH}_2$  radioconjugate because of nontarget retention. **Conclusion:** The pharmacokinetic and small-animal PET/CT studies demonstrate significantly improved nontarget tissue clearance for the  $^{64}\text{Cu}$ -CB-TE2A-8-AOC-BBN(7–14) $\text{NH}_2$ . This is attributed to the improved in vivo stability of the  $^{64}\text{Cu}$ -CB-TE2A chelate complex as compared with the  $^{64}\text{Cu}$ -DOTA chelate complex.

**Key Words:** BB2 receptor; bombesin;  $^{64}\text{Cu}$ ; preclinical; prostate cancer

**J Nucl Med 2007; 48:1327–1337**  
DOI: 10.2967/jnumed.107.039487

**T**he bombesin family of receptors—in particular, the BB2 receptor—has received a great deal of attention as a potential target for target-directed radiopharmaceuticals due to the high densities of these receptors on a variety of human tumors (1–3). The BB2 receptor subtype has been the most thoroughly studied receptor of the bombesin family and has been shown to be overexpressed in prostate, breast, small cell lung, and pancreatic cancers. Bombesin (BBN) is a 14-amino acid amphibian peptide that has been shown to bind to the BB2 receptor with high affinity (4). Our group and others have been involved in the synthesis of bombesin analogs that incorporate a radionuclide into the structure of the bombesin peptide (5–13). These radiolabeled analogs have been shown to target the BB2 receptor in vivo with high affinity. The potential of bombesin analogs for targeting the BB2 receptors overexpressed on prostate and breast cancer has been demonstrated in human clinical trials by Van de Wiele et al. and others (14–18). Research to find analogs that have optimal retention and clearance properties for diagnostic imaging and radionuclide therapeutic applications continues.

Received Jan. 9, 2007; revision accepted Apr. 23, 2007.

For correspondence or reprints contact: Timothy J. Hoffman, PhD, Harry S. Truman Veterans' Hospital, 800 Hospital Dr. F-003, Columbia, MO 65201-5275.

E-mail: HoffmanT@health.missouri.edu

COPYRIGHT © 2007 by the Society of Nuclear Medicine, Inc.

$^{64}\text{Cu}$  (half-life [ $t_{1/2}$ ] = 12.7 h) is a radionuclide that has received a great deal of interest for both diagnostic imaging and radionuclide therapy due to the radionuclide's dual decay characteristics. The positron ( $\beta^+$ : 18%,  $E_{\beta^+ \text{max}}$  = 653 keV) and beta ( $\beta^-$ : 37%,  $E_{\beta^- \text{max}}$  = 578 keV) emissions of  $^{64}\text{Cu}$  could allow clinicians the potential to diagnostically image a patient using PET and, subsequently, give therapeutic treatment using the same  $^{64}\text{Cu}$ -targeted radiopharmaceutical. However, the widespread application of  $^{64}\text{Cu}$ -based radiopharmaceuticals has been hindered by the lack of in vivo stable copper radiotracers. The uptake and retention of copper-containing compounds in the blood and liver has been known for over half a century (19–24).

Acyclic and macrocyclic polyamines have been widely used as chelators due to the rapid formation of thermodynamically and kinetically inert complexes with a variety of medically useful metals. These chelation systems are used today with a great deal of success for stabilizing a variety of medicinal metals for a multitude of clinical applications. Acyclic and macrocyclic polyamines have had limited success stabilizing copper in vivo due to poor kinetic stability (25–27). Macrocyclic polyamine complexes of copper, such as 1,4,8,11-tetraazacyclotetradecane-*N,N',N'',N'''*-tetraacetic acid (TETA) and 1,4,7,10-tetraazacyclododecane-*N,N',N'',N'''*-tetraacetic acid (DOTA) have been shown to exhibit greater kinetic inertness than acyclic analogs, but significant transchelation still occurs (26,27). The design and synthesis of kinetically inert chelation moieties for copper nuclides and other medically relevant metals is currently an active area of research (28).

One of several new chelate designs for copper radionuclides focuses on cross-bridged tetraazamacrocycles. 1,4,8,11-Tetraazabicyclo[6.6.2]hexadecane-4,11-diacetic acid (CB-TE2A), reported by Wong et al. in 2000, is a cross-bridge derivative of the TETA macrocycle (29). The cross-bridged tetraamine bicycles were found to be an improvement over their monocyclic counterparts. The rigidity of the cross-bridge systems is accredited for the greater kinetic stability of the copper(II) cross-bridged complexes over traditional DOTA and TETA analogs. Recently, the collaborative work of the Anderson, Weisman, and Wong laboratories has yielded several reports with regard to the in vitro and in vivo properties of copper(II)-CB-TE2A (30–33). This collaboration also yielded the first  $^{64}\text{Cu}$  receptor-targeted radiopharmaceutical that incorporated a cross-bridged chelation system,  $^{64}\text{Cu}$ -CB-TE2A-Y3-TATE. Anderson et al. reported that the  $^{64}\text{Cu}$ -CB-TE2A conjugate poses significantly greater in vivo stability when compared directly with the  $^{64}\text{Cu}$ -TETA conjugate in an AR42J tumor-bearing rat model (32).

Our group has reported the synthesis and evaluation of a series of bombesin analogs of the type  $^{111}\text{In}$ -DOTA-X-BBN(7–14) $\text{NH}_2$ , where X = 0-, 3-, 5-, 8-, or 11-atom-length hydrocarbon spacers to determine the effect of spacer length on pharmacokinetics (5). From this work, the conjugates with the tethering lengths between 5 and 8

carbons,  $^{111}\text{In}$ -DOTA-5-AVA-BBN(7–14) $\text{NH}_2$  and  $^{111}\text{In}$ -DOTA-8-AOC-BBN(7–14) $\text{NH}_2$ , respectively, provided the most favorable pharmacokinetic properties. Using this paradigm, Rogers and coworkers recently reported the synthesis and evaluation of  $^{64}\text{Cu}$ -DOTA-8-AOC-BBN(7–14) $\text{NH}_2$  (9,34). The  $^{64}\text{Cu}$ -DOTA-8-AOC-BBN(7–14) $\text{NH}_2$  radioconjugate demonstrated good uptake and impressive retention in the PC-3 tumor mouse model, but the pharmacokinetic properties are indicative of the in vivo instability of  $^{64}\text{Cu}$  tetraazamacrocyclic chelates (i.e., transchelation to advantageous proteins).

The purpose of the current study was to directly compare bombesin analogs synthesized with the CB-TE2A chelator with traditional tetraazamacrocyclic conjugates for in vivo stability. The  $^{64}\text{Cu}$ -CB-TE2A-8-AOC-BBN(7–14) $\text{NH}_2$  radioconjugate and the previously reported  $^{64}\text{Cu}$ -DOTA-8-AOC-BBN(7–14) $\text{NH}_2$  radioconjugate were synthesized for the purpose of a direct side-by-side comparison. Here, we present the synthesis of the  $^{64}\text{Cu}$ -CB-TE2A-8-AOC-BBN(7–14) $\text{NH}_2$  and  $^{64}\text{Cu}$ -DOTA-8-AOC-BBN(7–14) $\text{NH}_2$  radioconjugates and the in vitro and in vivo evaluation and characterization using small-animal PET technology.

## MATERIALS AND METHODS

Unless otherwise specified, all chemicals and reagents were used as received.  $^{64}\text{Cu}$  was purchased from MDS Nordion. Fmoc-protected amino acids and resins were purchased from EMD Biosciences Inc. Tris (1,1-dimethylethyl)-1,4,7,10-tetraazacyclododecane-1,4,7,10-tetraacetic acid was purchased from Macrocyclics. 1,4,8,11-Tetraazabicyclo[6.6.2]hexadecane-4,11-diacetic acid was prepared according to literature procedures (29,35,36). Fmoc-8-Aminooctanoic acid was purchased from Advanced ChemTech. Naturally abundant copper(II) sulfate pentahydrate, *N,N*-dimethylformamide (DMF), *N*-methyl-2-pyrrolidone (NMP), and diisopropylethylamine (DIEA) were purchased from Fischer Scientific. HPLC (high-performance liquid chromatography)-grade acetonitrile and trifluoroacetic acid were purchased from Fischer Scientific for HPLC analyses. Deionized water used for HPLC analyses and all other chemical applications in this work was obtained from an in-house Millipore Milli-Q Biocel water purification system. RPMI 1640 medium was purchased from Invitrogen/GIBCO. 4-(2-Hydroxyethyl)-1-piperazineethanesulfonic acid (HEPES) and bovine serum albumin (BSA) were purchased from Fisher Scientific (Fisher Bioreagents, Fisher Chemical). [ $^{125}\text{I}$ -Tyr $^4$ ]BBN (370 kBq [10  $\mu\text{Ci}$ ]) was purchased from Perkin Elmer.

Solid-phase peptide synthesis (SPPS) was performed using an Applied Biosystems model 432 automated peptide synthesizer using standard Fmoc chemistry. Reversed-phase HPLC (RP-HPLC) purification of the conjugates,  $^{nat}\text{Cu}$ -conjugates and  $^{64}\text{Cu}$ -conjugates, was accomplished using a Waters 600E controller equipped with an Eppendorf TC-50 column heater. A Phenomenex Jupiter 5- $\mu\text{m}$   $\text{C}_{18}$  300- $\text{\AA}$ , 250  $\times$  10 mm semipreparative column was used for the purification of bulk amounts of CB-TE2A-8-AOC-BBN(7–14) $\text{NH}_2$ . A Phenomenex Jupiter 5- $\mu\text{m}$   $\text{C}_{18}$  300- $\text{\AA}$ , 250  $\times$  4.6 mm analytic column was used for the purification of all conjugates for in vitro and in vivo studies. Detection of the conjugates and  $^{nat}\text{Cu}$ -conjugates during HPLC purification was accomplished using a JASCO UV 975 absorbance detector, whereas the radioconjugates were detected during HPLC purification using a JASCO UV 1575

absorbance detector and an ORTEC (Oak Ridge National Laboratory) NaI(Tl) scintillation detector. During the preparation of the radioconjugates, 3M Empore High Performance Extraction Disk Cartridges 4215(HD) were used. Mass spectrometric determination of the conjugates and  $^{nat}\text{Cu}$  conjugates was achieved by nanospray time-of-flight mass spectrometry (QqTOF MS) using an Applied Biosystems/MDS Sciex QStar/Pulsar/i instrument. Radiation measurements for the in vitro binding studies were accomplished using the Packard Riasar  $\gamma$ -counter. Pharmacokinetic radiation measurements were made using a well counter equipped with a NaI(Tl) scintillation detector.

Four- to 5-wk-old ICR SCID (Institute of Cancer Research severely compromised immunodeficient) female mice were obtained from Taconic Farms. The mice were supplied with sterilized water and irradiated rodent chow (Ralston Purina Co.) ad libitum. Five mice were housed per microisolator cage (Alternative Design) in a humidity- and temperature-controlled room with a 12-h light/dark cycle. The human prostate cancer PC-3 cell line was purchased from the American Type Culture Collection. The PC-3 cell line was grown and maintained by the University of Missouri Cell and Immunobiology Core Facility. PC-3 cells were grown in custom RPMI medium 1640 (Invitrogen Corp.) supplemented with 10% fetal bovine serum (U.S. Bio-Technologies Inc.) and gentamicin (American Pharmaceutical Partners, Inc.). To prepare the cells for inoculation, the PC-3 cells with media were centrifuged, the media was decanted, and the cell pellet was combined with Dulbecco's phosphate-buffered saline (Invitrogen Corp.) to reach a concentration of 5 million cells/100  $\mu\text{L}$ . Under gas anesthesia, each SCID mouse was subcutaneously inoculated (bilateral flank) with 5 million PC-3 tumor cells in each flank. Using a nonrebreathing apparatus (Summit Medical Equipment Co.), gas anesthesia was administered at a vaporizer setting of  $\sim 3.5\%$  isoflurane (Baxter Healthcare Corp.) with  $\sim 1$  L/min oxygen. The flank tumors were allowed to grow for 3–4 wk before studies were performed. All studies involving animals were conducted in accordance with protocols approved by the institutional animal care and use committee in accordance with U.S. Public Health Service guidelines.

## SPPS

The conjugates were assembled using automated peptide synthesis. The crude conjugate was dried by vacuum, weighed, and analyzed by RP-HPLC. Purity of the crude peptides, as determined by RP-HPLC, varied depending on the conjugate. For DOTA-8-AOC-BBN(7–14) $\text{NH}_2$ , the unpurified peptide was determined to be 70% pure by HPLC. The synthesis of CB-TE2A-8-AOC-BBN(7–14) $\text{NH}_2$  was found to be more problematic, with purity determinations of 10% by HPLC. Due to the low yields for CB-TE2A-8-AOC-BBN(7–14) $\text{NH}_2$ , the conjugate was purified using semipreparative RP-HPLC before studies were performed. All conjugates were peak purified to  $\geq 93\%$  purity and quantified by analytic RP-HPLC before mass spectrometric determination and in vitro studies. Confirmation of the desired conjugates' constitution was determined by mass spectrometry.

## Syntheses of $^{nat}\text{Cu}$ -Conjugates

For DOTA-8-AOC-BBN(7–14) $\text{NH}_2$  and CB-TE2A-8-AOC-BBN(7–14) $\text{NH}_2$ , a 1-mg sample of the conjugate was dissolved in 500  $\mu\text{L}$  of a 0.1 M ammonium acetate/0.80 mM copper(II) sulfate pentahydrate solution. The solutions were heated at  $70^\circ\text{C}$  for 40 min and allowed to cool to room temperature.  $^{nat}\text{Cu}$ -

Conjugates were then peak purified and quantified by RP-HPLC. All  $^{nat}\text{Cu}$ -conjugates were determined to be  $\geq 93\%$  pure, by RP-HPLC analyses before mass spectrometric characterization and in vitro binding studies.

## Radiolabeling of Conjugates with $^{64}\text{CuCl}_2$

A 100- $\mu\text{g}$  sample of the conjugate and  $\sim 20$  mg of L-ascorbic acid (radiolysis prevention reagent) were dissolved in 200  $\mu\text{L}$  of 0.4 M ammonium acetate (pH 7.0).  $^{64}\text{CuCl}_2$  was added to the vial containing the conjugate, and the solution was heated for 40 min at  $70^\circ\text{C}$  and allowed to cool to room temperature. The resulting  $^{64}\text{Cu}$ -radioconjugate was peak purified using RP-HPLC. The peak-purified  $^{64}\text{Cu}$ -radioconjugate was concentrated using a C<sub>18</sub> extraction disk and eluted with 400  $\mu\text{L}$  of a 6:4 ethanol/sterile saline solution. For pharmacokinetic studies, the purified  $^{64}\text{Cu}$ -conjugates were diluted with sterile saline to 0.185 MBq (5  $\mu\text{Ci}$ ) per 100  $\mu\text{L}$ . Imaging studies required evaporation of the ethanol from the  $^{64}\text{Cu}$ -radioconjugate solution under a stream of nitrogen and dilution to the appropriate volume with sterile saline solution. In all cases, the concentration of ethanol in solution was  $< 8\%$  before administration. The radiochemical yield for  $^{64}\text{Cu}$ -DOTA-8-AOC-BBN(7–14) $\text{NH}_2$  averaged 68% by HPLC, whereas that for  $^{64}\text{Cu}$ -CB-TE2A-8-AOC-BBN(7–14) $\text{NH}_2$  averaged 30%. The radiochemical purity of all  $^{64}\text{Cu}$ -radioconjugates for pharmacokinetic and imaging studies was reassessed before administration and found to be  $\geq 93\%$  pure.

## HPLC Purification and Analyses

Bulk sample purification of CB-TE2A-8-AOC-BBN(7–14) $\text{NH}_2$  was performed using a semipreparative column with a flow rate of 5.0 mL/min. Sample purification for mass spectrometric in vitro and in vivo studies was performed on an analytic column with a flow rate of 1.5 mL/min. For all HPLC experiments, the mobile phase consisted of solvent A (99.9%  $\text{H}_2\text{O}$  and 0.1% trifluoroacetic acid [TFA]) and solvent B (99.9%  $\text{CH}_3\text{CN}$  and 0.1% TFA). For all conjugates,  $^{nat}\text{Cu}$ -conjugates and  $^{64}\text{Cu}$ -conjugates, the gradient began at 80% A:20% B and over a period of 15 min linearly decreased to a gradient of 70% A:30% B. At the end of the 15-min run time for all HPLC experiments, the column was flushed with the gradient 5% A:95% B and reequilibrated to the starting gradient.

## In Vitro Competitive Cell-Binding Studies

Fifty-percent inhibitory concentration ( $\text{IC}_{50}$ ) binding studies for all conjugates and  $^{nat}\text{Cu}$ -conjugates were performed using PC-3 human prostate cancer cells.  $^{nat}\text{Cu}$ -conjugates were used to determine the specific binding affinities for the corresponding  $^{64}\text{Cu}$ -conjugates. Cell media consisted of RPMI medium at pH 7.4, 4.8 mg/mL HEPES, and 2 mg/mL BSA. For binding assays, the cells ( $\sim 3 \times 10^4$  PC-3 cells) were suspended in media and incubated at  $37^\circ\text{C}$  for 40 min in the presence of radiolabeled [ $^{125}\text{I}$ -Tyr<sup>4</sup>]BBN, a known BB2 agonist, and a range of concentrations of the conjugate or  $^{nat}\text{Cu}$ -conjugate. After incubation, the cells were aspirated and washed (3 $\times$ ) with media. The cell-associated activity was measured, and the binding affinity was determined.

## Internalization Assays

Internalization studies were performed by incubating  $3 \times 10^4$  PC-3 human prostate cancer cells in cell media. The cell medium consisted of RPMI medium with 2 mg/mL BSA and 2.8 mg/mL HEPES at pH 7.4. The cells were incubated at  $37^\circ\text{C}$  with 20,000 cpm of the  $^{64}\text{Cu}$ -CB-TE2A-8-AOC-BBN(7–14) $\text{NH}_2$  in the presence



of 5% CO<sub>2</sub> for 15-, 30-, 45-, 60-, and 120-min time points. At the end of that time point, binding was halted by aspiration of the cell medium and washing of the cells (3×) with ice-cold cell culture medium. Surface-bound radioactivity was removed from the cellular membrane surface by addition of ice-cold pH 2.5 saline buffer (0.2 mol/L acetic acid and 0.5 mol/L NaCl). The cells were vortexed and incubated in the medium for 5 min, followed by the removal of the radioactivity in the supernatant by aspiration and washing the cells (2×) with pH 2.5 saline buffer. The radioactivity was determined for the supernatant and the cells as a function of time, which yielded the percentage radioactivity surface bound and internalized, respectively. Analogous studies were performed with <sup>64</sup>Cu-DOTA-8-AOC-BBN(7–14)NH<sub>2</sub> at 15-, 30-, 45-, 60-, 90-, and 120-min time points.

### Pharmacokinetic Studies of <sup>64</sup>Cu-Radioconjugates in PC-3 Xenograft SCID Mice

The PC-3 tumor-bearing SCID mice used in pharmacokinetic studies were allowed to grow tumors, which ranged from 0.2 to 1.0 g (3–4 wk after inoculation). Pharmacokinetic studies involving the <sup>64</sup>Cu-radioconjugates were performed using age-matched SCID mice. Each mouse (average weight, 25 g) received a tail vein bolus of 0.185 MBq (5 μCi) of the radio-RP-HPLC peak-purified <sup>64</sup>Cu-radioconjugate in 100 μL of saline. The mice were sacrificed and their tissues and organs were excised at 15-min, 1-h, 4-h, and 24-h time points after injection. The excised tissues were weighed, the tissue activity was measured, and the percentage injected dose (%ID) and percentage injected dose per gram (%ID/g) were determined for each tissue. Whole-blood %ID and %ID/g were determined assuming the blood accounted for 6.5% of the body weight of the mouse. In vivo receptor blocking for the <sup>64</sup>Cu-CB-TE2A radioconjugate was performed using 100 μg of BBN coadministered with ~0.185 MBq (~5 μCi) of the <sup>64</sup>Cu-CB-TE2A radioconjugate.

### microPET/microCT Studies

microPET imaging was performed using a MOSAIC small-animal PET unit (Philips, USA). The unit has a gantry diameter of 21 cm, a transverse field of view (FOV) of 12.8 cm, and an axial length of 11.6 cm. The scanner operates in a 3-dimensional (3D) volume imaging acquisition mode. Small animals are laser aligned at the center of the scanner FOV for subsequent imaging. Mouse microPET studies were performed using 40.7 MBq (1.10 mCi) and 38.1 MBq (1.03 mCi) of the <sup>64</sup>Cu-DOTA and <sup>64</sup>Cu-CB-TE2A radioconjugates, respectively. The mice were sacrificed at 20 h after administration of the radioconjugates. microPET image reconstruction was performed with a 3D row-action maximum-likelihood algorithm (RAMLA) without tissue attenuation correction. microCT was performed immediately after microPET for the purpose of anatomic/molecular data fusion. microCT was acquired in approximately 8 min, and concurrent image reconstruction was achieved using a Fanbeam (Feldkamp) filtered-backprojection algorithm. Reconstructed DICOM (digital imaging and communication in medicine) PET images with a matrix size of 256 × 256 × 240 and a voxel size of 0.125 mm<sup>3</sup> were imported into AMIRA 3.1 software (Mercury) for subsequent image fusion with microCT and 3D visualization. PET images were filtered after reconstruction using a gaussian filter and normalized to each other by identifying pixel intensity using a maximum-intensity-projection rendering method to visualize high-intensity structures within volumetric data.

## RESULTS

CB-TE2A was largely prepared according to the literature procedures of Wong, Weisman, and coworkers (29,36). *cis*-Decahydro-1*H*,6*H*-3*a*,5*a*,8*a*,10*a*-tetraazapyrene, the precursor of CB-TE2A, was prepared according to the method of Le Baccon et al. (35). The CB-TE2A was isolated and stored as the tetrahydrochloride salt (CB-TE2A·4HCl). The free base of the salt was synthesized before use.

The CB-TE2A-8-AOC-BBN(7–14)NH<sub>2</sub> and DOTA-8-AOC-BBN(7–14)NH<sub>2</sub> conjugates, depicted in Figure 1, were prepared by SPSS using standard Fmoc and orthogonal protection schemes. The poor solubility of the CB-TE2A·4HCl in DMF prevented loading of the chelator directly onto the automatic peptide synthesizer. Instead, a suspension of the tetrahydrochloride salt in a 3:1 DMF:2.0 M DIEA in NMP mixture was prepared. Excess diisopropylethylamine was slowly added to the mixture and the solution was allowed to stir for 1 h. The mixture was filtered and loaded manually onto the automatic peptide synthesizer. The synthesis was completed using standard activation and coupling chemistry. The above synthetic preparation of CB-TE2A-8-AOC-BBN(7–14)NH<sub>2</sub> typically yielded a crude product that, on average, was found to be 10% pure, as determined by RP-HPLC. Inefficient coupling of the CB-TE2A chelator to the growing peptide was found to be responsible for the poor yield. Studies to improve the yield of the CB-TE2A conjugate are currently underway. The crude product was peak purified using semipreparative RP-HPLC. The DOTA-8-AOC-BBN(7–14)NH<sub>2</sub> conjugate was prepared according to procedures first reported by Hoffman et al. (5). Mass spectrometric confirmation and RP-HPLC retention times of the conjugates are listed in Table 1.

Nonradioactive Cu-DOTA-8-AOC-BBN(7–14)NH<sub>2</sub> and Cu-CB-TE2A-8-AOC-BBN(7–14)NH<sub>2</sub> conjugates (Fig. 1) were synthesized by heating aqueous solutions of the conjugate and CuSO<sub>4</sub>·5H<sub>2</sub>O at 70°C for 40 min. Copper conjugates were purified by RP-HPLC and determined to be ≥93% pure before being analyzed by mass spectrometry and undergoing in vitro cell-binding assays. Mass spectrometric and RP-HPLC retention times of the copper conjugates are given in Table 1. The coordination sphere around the copper atom in Cu-CB-TE2A-BBN(7–14)NH<sub>2</sub> is 6 coordinate, with 4 nitrogen donors from the bicyclic macrocycle and a carboxylate and an amide group to balance the dicationic charge of the copper. The depiction of the Cu-CB-TE2A-8-AOC-BBN(7–14)NH<sub>2</sub> conjugate is consistent with mass spectrometric data.

<sup>64</sup>Cu-DOTA-8-AOC-BBN(7–14)NH<sub>2</sub> and <sup>64</sup>Cu-CB-TE2A-8-AOC-BBN(7–14)NH<sub>2</sub> were synthesized using a slightly modified procedure of that reported by Rogers et al. (9). DOTA-8-AOC-BBN(7–14)NH<sub>2</sub> or CB-TE2A-8-AOC-BBN(7–14)NH<sub>2</sub> was dissolved in 0.4 M ammonium acetate (pH 7.0), and <sup>64</sup>CuCl<sub>2</sub> was added to the solution. The solution was heated for 40 min at 70°C. The retention times of <sup>64</sup>Cu-DOTA-8-AOC-BBN(7–14)NH<sub>2</sub> and <sup>64</sup>Cu-CB-TE2A-8-AOC-BBN(7–14)NH<sub>2</sub> were 15.8 and 17.2 min, respectively, under

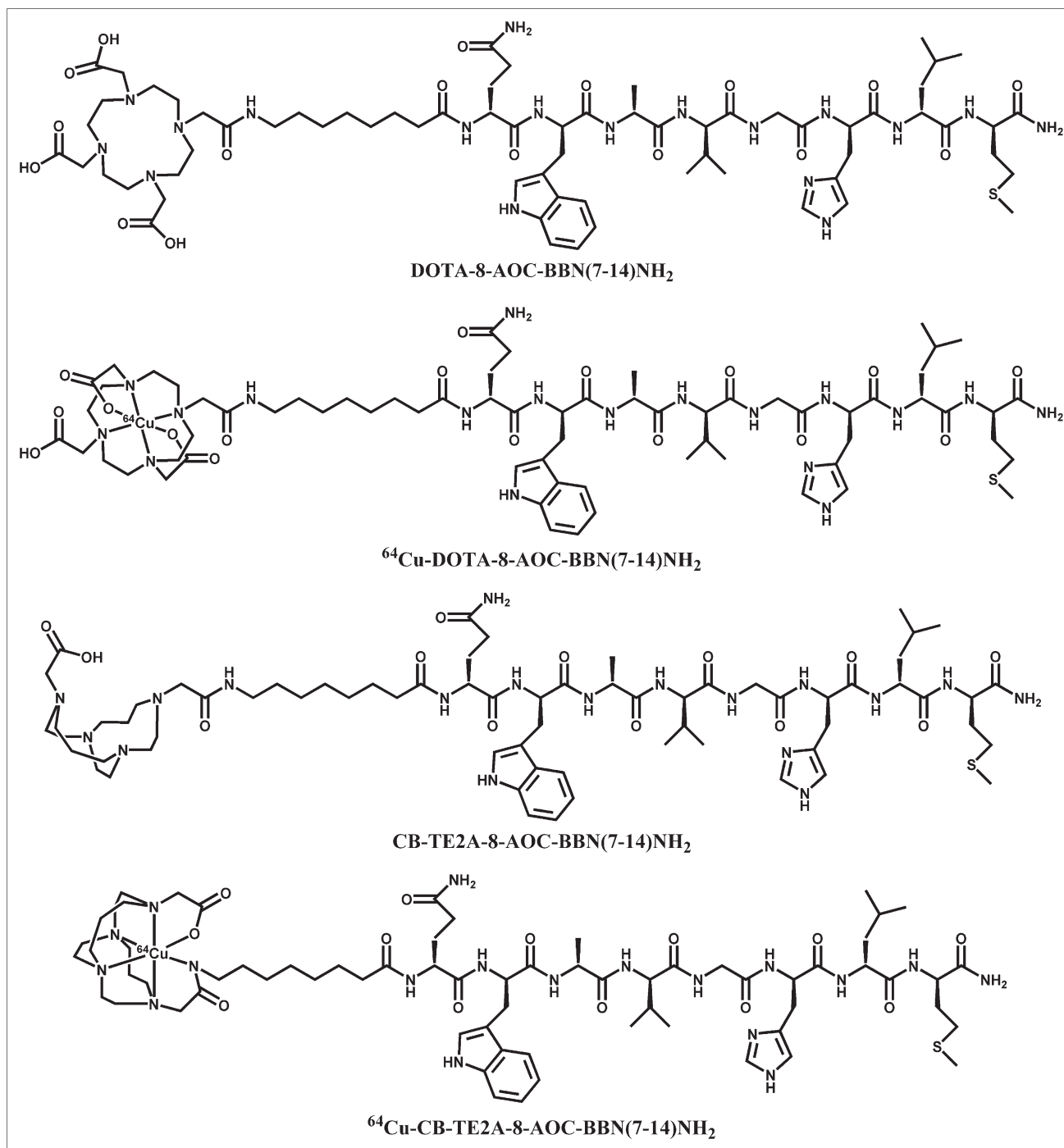


**FIGURE 1.** Structure of bombesin and <sup>64</sup>Cu-labeled bombesin analogs.

identical RP-HPLC conditions. The radiochemical yields of <sup>64</sup>Cu-DOTA-8-AOC-BBN(7-14)NH<sub>2</sub> and <sup>64</sup>Cu-CB-TE2A-8-AOC-BBN(7-14)NH<sub>2</sub> were 68% and 30%, respectively.

In vitro competitive binding studies of the conjugates and nonradioactive copper conjugates were performed (Table 1) using PC-3 cells. The competitive binding curves for <sup>nat</sup>Cu-CB-TE2A-8-AOC-BBN(7-14)NH<sub>2</sub> and <sup>nat</sup>Cu-DOTA-8-AOC-BBN(7-14)NH<sub>2</sub> are shown in Figure 2 with competition

against [<sup>125</sup>I-Tyr<sup>4</sup>]BBN, a peptide known to bind to the BB2 receptor with high affinity. Both of the copper conjugates demonstrated nanomolar binding affinity for the BB2 receptor with little nonspecific binding.

Incubation of PC-3 cells with <sup>64</sup>Cu-CB-TE2A-8-AOC-BBN(7-14)NH<sub>2</sub> and <sup>64</sup>Cu-DOTA-8-AOC-BBN(7-14)NH<sub>2</sub> is shown in Figures 3 and 4, respectively. For the <sup>64</sup>Cu-CB-TE2A radioconjugate, the amount of internalized activity

**TABLE 1**  
Mass Spectrometric, RP-HPLC, and In Vitro IC<sub>50</sub> Characterization of Conjugates

Analog	Molecular formula	MS calculated	MS observed	RP-HPLC t <sub>r</sub> (min)*	IC <sub>50</sub> (nM) <sup>†</sup>
DOTA-8-AOC-BBN(7–14)NH <sub>2</sub>	C <sub>67</sub> H <sub>106</sub> N <sub>18</sub> O <sub>17</sub> S	1,467.8	1,468.0	13.8	
Cu-DOTA-8-AOC-BBN(7–14)NH <sub>2</sub>	C <sub>67</sub> H <sub>104</sub> N <sub>18</sub> O <sub>17</sub> SCu	1,528.7	1,528.5	15.0	1.44 ± 0.08
CB-TE2A-8-AOC-BBN(7–14)NH <sub>2</sub>	C <sub>67</sub> H <sub>108</sub> N <sub>18</sub> O <sub>13</sub> S	1,405.8	1,405.8	15.8	0.67 ± 0.07
Cu-CB-TE2A-8-AOC-BBN(7–14)NH <sub>2</sub>	C <sub>67</sub> H <sub>106</sub> N <sub>18</sub> O <sub>13</sub> SCu	1,465.7	1,465.7	17.2	0.48 ± 0.01

\*RP-HPLC methods described in Materials and Methods.

<sup>†</sup>In vitro binding assays were performed in triplicate.

exceeded the amount of surface-associated activity. Rapid uptake of the radioconjugate was observed for the first 15 min of incubation. After 15 min of incubation, the <sup>64</sup>Cu-CB-TE2A radioconjugate was internalized at a steadily increasing rate for the remaining time points of the internalization assay. For the <sup>64</sup>Cu-DOTA radioconjugate, the amount of surface-bound activity equaled or exceeded the amount of internalized activity at all time points. Similar to the <sup>64</sup>Cu-CB-TE2A radioconjugate, internalization of the <sup>64</sup>Cu-DOTA radioconjugate showed a steady rate of accumulation of activity in the cell over the time of the study.

The results obtained from pharmacokinetic studies of <sup>64</sup>Cu-DOTA-8-AOC-BBN(7–14)NH<sub>2</sub> and <sup>64</sup>Cu-CB-TE2A-8-AOC-BBN(7–14)NH<sub>2</sub> in SCID mice bearing PC-3 xenografts are summarized in Tables 2 and 3, respectively. A comparison of the tumor-to-nontarget tissue ratios of the 2 radioconjugates in selected nontarget tissues is depicted in Figure 5. The pharmacokinetic values for the <sup>64</sup>Cu-DOTA-8-AOC-BBN(7–14)NH<sub>2</sub> radioconjugate agree well with analogous literature time points reported by Rogers et al. (9). Overall, the <sup>64</sup>Cu-CB-TE2A-8-AOC-BBN(7–14)NH<sub>2</sub> radioconjugate showed significantly better clearance from the

mouse model than the <sup>64</sup>Cu-DOTA-8-AOC-BBN(7–14)NH<sub>2</sub> radioconjugate. At 24 h after injection, 98.60 ± 0.28 %ID had been excreted from the mice using the <sup>64</sup>Cu-CB-TE2A-8-AOC-BBN(7–14)NH<sub>2</sub> radioconjugate compared with only 67.84 ± 5.43 %ID using the <sup>64</sup>Cu-DOTA-8-AOC-BBN(7–14)NH<sub>2</sub> radioconjugate. Overall clearance of both <sup>64</sup>Cu bombesin analogs proceeded mostly through the renal system, with approximately 20 %ID being excreted through the hepatobiliary system.

The <sup>64</sup>Cu-CB-TE2A-8-AOC-BBN(7–14)NH<sub>2</sub> radioconjugate clears more efficiently from the bloodstream than the <sup>64</sup>Cu-DOTA radioconjugate. At 24 h after injection, the retention in the blood was 0.07 ± 0.05 and 1.40 ± 0.84 %ID for the <sup>64</sup>Cu-CB-TE2A and <sup>64</sup>Cu-DOTA radioconjugates, respectively. For the <sup>64</sup>Cu-DOTA-8-AOC-BBN(7–14)NH<sub>2</sub> radioconjugate, retention of <sup>64</sup>Cu in the liver was found to be 7.80 ± 1.51 %ID/g at 24 h after injection. The <sup>64</sup>Cu-CB-TE2A radioconjugate shows superior clearance from the liver, with 0.21 ± 0.06 %ID/g remaining at 24 h after injection. Initial tumor uptake of the two <sup>64</sup>Cu bombesin analogs shows statistically the same activity at 15 min after injection. However, the <sup>64</sup>Cu-DOTA-8-AOC-BBN(7–14)NH<sub>2</sub> radioconjugate showed significantly higher retention compared with the <sup>64</sup>Cu-CB-TE2A-8-AOC-BBN(7–14)NH<sub>2</sub> radioconjugate. At 24 h after injection, the tumor activity (3.88 ± 1.40 %ID/g) using the <sup>64</sup>Cu-DOTA radioconjugate is statistically the same as the tumor uptake at 15-min, 1-h, and 4-h time points after injection. Despite the tumor retention of the <sup>64</sup>Cu-DOTA radioconjugate, the tumor-to-liver, tumor-to-blood, and tumor-to-kidney ratios were found to be higher for the <sup>64</sup>Cu-CB-TE2A radioconjugate at all time points due to the relative clearance of the radioconjugate from nontarget tissue. The tumor-to-muscle ratios were found to be greater for the <sup>64</sup>Cu-CB-TE2A radioconjugate with the exception of the 24-h time point after injection. The significant retention of the <sup>64</sup>Cu-DOTA radioconjugate and clearance of the <sup>64</sup>Cu-CB-TE2A radioconjugate from the tumors results in a higher tumor-to-muscle ratio for the <sup>64</sup>Cu-DOTA radioconjugate at the 24-h time point after injection. Blocking studies were performed with 100 μg of BBN coadministered with the <sup>64</sup>Cu-CB-TE2A radioconjugate. As demonstrated with other bombesin analogs, the blocking studies for the <sup>64</sup>Cu-CB-TE2A radioconjugate demonstrated significant BB2 receptor blocking (95%)

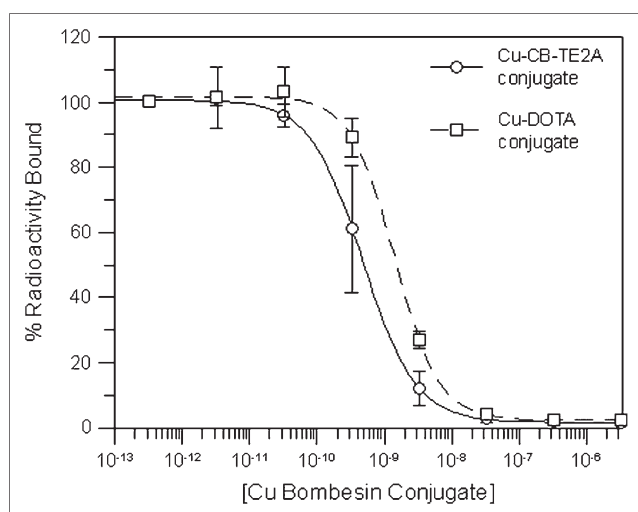


**FIGURE 2.** Competitive binding assay of Cu-DOTA-8-AOC-BBN(7–14)NH<sub>2</sub> and Cu-CB-TE2A-8-AOC-BBN(7–14)NH<sub>2</sub> analogs vs. [<sup>125</sup>I-Tyr<sup>4</sup>]BBN using PC-3 cells (*n* = 3).

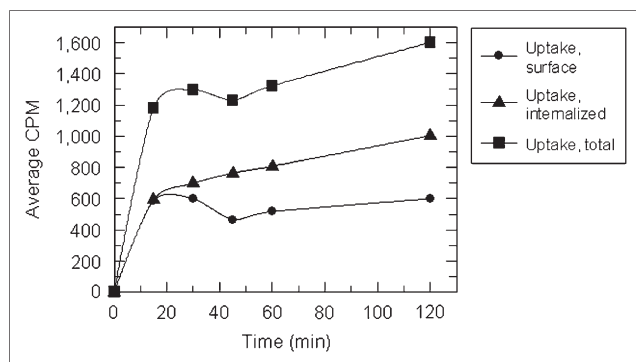


**FIGURE 3.** Internalization of  $^{64}\text{Cu}$ -CB-TE2A-8-AOC-BBN(7-14) $\text{NH}_2$  using PC-3 cells ( $n = 6$ ).

in the BB2 receptor-rich mouse pancreas. The tumor uptake was also blocked and is consistent with blocking studies of other bombesin analogs.

microPET, fused microPET/CT, and axial images of PC-3 tumor-bearing SCID mice using  $^{64}\text{Cu}$ -DOTA-8-AOC-BBN(7-14) $\text{NH}_2$  and  $^{64}\text{Cu}$ -CB-TE2A-8-AOC-BBN(7-14) $\text{NH}_2$  radioconjugates are shown in Figure 6. The images of both conjugates at 20 h after injection correlate well with respective pharmacokinetic studies at 24 h after injection. For both radioconjugates, the BB2 receptor-mediated uptake in the tumors can be easily visualized in the axial images at the 20-h time point after injection. For the  $^{64}\text{Cu}$ -DOTA radioconjugate, substantial abdominal uptake and retention—in particular, the liver, kidneys, and gastrointestinal tract—are clearly evident. Images of the  $^{64}\text{Cu}$ -CB-TE2A-8-AOC-BBN(7-14) $\text{NH}_2$  radioconjugate show substantially less abdominal activity relative to the  $^{64}\text{Cu}$ -DOTA radioconjugate. The most striking difference in the 2 whole-body images is the significantly reduced accumulation in the liver using the  $^{64}\text{Cu}$ -CB-TE2A radioconjugate.

## DISCUSSION

Copper radioisotopes have been shown to transchelate from chelation systems, including the DOTA and TETA

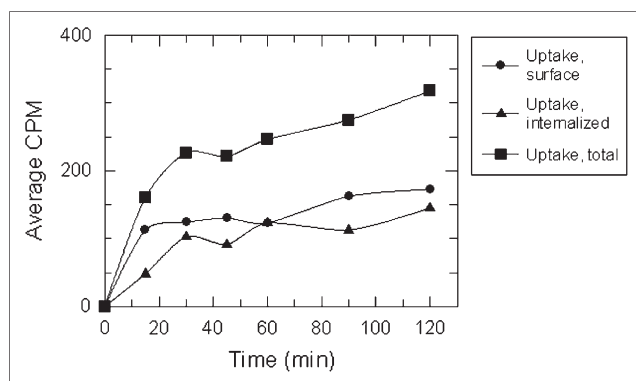


**FIGURE 4.** Internalization of  $^{64}\text{Cu}$ -DOTA-8-AOC-BBN(7-14) $\text{NH}_2$  using PC-3 cells ( $n = 2$ ).

tetraamine macrocycles, and bind to proteins, including serum albumin and superoxide dismutase. The reduction of  $\text{Cu(II)}$  to  $\text{Cu(I)}$  has been suggested to be the source of the kinetic instability (33,37). If this rationale is true, the chelator, on copper reduction, becomes unsuitable for the labile copper(I) species and transchelation occurs. A recent report by Weisman and coworkers investigates the electrochemical in vitro properties of tetraazamacrocycles and cross-bridge tetraazabicycles (33). Their work suggests that the CB-TE2A chelator can stabilize both copper(I) and copper(II) species—assuming copper reduction is the primary reason for transchelation—thereby significantly reducing transchelation due to copper reduction.

Under the radiolabeling conditions used in this work, the CB-TE2A conjugate was found to be more difficult to radiolabel than the DOTA conjugate. The radiochemical yield of the  $^{64}\text{Cu}$ -CB-TE2A-8-AOC-BBN(7-14) $\text{NH}_2$  radioconjugate was approximately half that of the  $^{64}\text{Cu}$ -DOTA-8-AOC-BBN(7-14) $\text{NH}_2$  radioconjugate. The difficulty in radiolabeling the CB-TE2A chelator has been previously noted (31,32). More vigorous labeling conditions may be required to achieve more optimal radiolabeling yields.

In vitro binding studies revealed a slightly higher binding affinity to the BB2 receptor for the Cu-CB-TE2A radioconjugate ( $\text{IC}_{50} = 0.48 \pm 0.01 \text{ nM}$ ) than the Cu-DOTA radioconjugate ( $\text{IC}_{50} = 1.44 \pm 0.08 \text{ nM}$ ). Internalization studies of the radioconjugates demonstrated a higher internalized-to-surface-bound ratio for the  $^{64}\text{Cu}$ -CB-TE2A radioconjugate. However, both conjugates demonstrated a steady increase in the concentration of activity in the cell over time. This trend is in agreement with internalization studies of the  $^{64}\text{Cu}$ -DOTA conjugate performed by Rogers and colleagues as well as the analogous  $^{111}\text{In}$ -DOTA-8-AOC-BBN(7-14) $\text{NH}_2$  radioconjugate reported by our group (5,9).

The tumor uptake for the  $^{64}\text{Cu}$ -CB-TE2A and  $^{64}\text{Cu}$ -DOTA radioconjugates was  $6.95 \pm 2.27$  and  $4.95 \pm 0.91 \text{ \%ID/g}$ , respectively, at 15 min after injection. Pharmacokinetic studies have been reported for several radiometals— $^{111}\text{In}$ ,  $^{177}\text{Lu}$ ,  $^{90}\text{Y}$ , and  $^{149}\text{Pm}$ —using the DOTA-8-AOC-BBN(7-14) $\text{NH}_2$  peptide (5,7,38,39). In these studies, the radiometal was found to have high initial uptake in the tumor (e.g.,  $^{111}\text{In}$ :  $7.59 \pm 2.11 \text{ \%ID/g}$  at 15 min after injection) and significant clearance of the radioactivity from the tumor over time (e.g.,  $^{111}\text{In}$ :  $1.56 \pm 0.45 \text{ \%ID/g}$  at 24 h after injection). The  $^{64}\text{Cu}$ -CB-TE2A-8-AOC-BBN(7-14) $\text{NH}_2$  radioconjugate demonstrated significant clearance from the tumor, with  $0.28 \pm 0.21 \text{ \%ID/g}$  or 4% of the 15-min value remaining at 24 h after injection. The retention profile of the  $^{64}\text{Cu}$ -CB-TE2A radioconjugate is consistent with previously reported radiometal complexes of DOTA-8-AOC-BBN(7-14) $\text{NH}_2$ . In contrast,  $^{64}\text{Cu}$ -DOTA-8-AOC-BBN(7-14) $\text{NH}_2$  demonstrated high retention and essentially no clearance from tumor tissue, with  $3.48 \pm 0.90$ ,  $3.00 \pm 1.10$ , and  $3.88 \pm 1.40 \text{ \%ID/g}$  at 1, 4, and 24 h after injection, respectively. The tumor tissue clearance profile of the  $^{64}\text{Cu}$ -DOTA radioconjugate suggests the retention is due to a nonreversible trapping mechanism, such as



**TABLE 2**  
In Vivo Pharmacokinetic Studies of  $^{64}\text{Cu}$ -DOTA-8-AOC-BBN(7–14) $\text{NH}_2$  Using SCID Mice Bearing PC-3 Xenografts

Tissue/organ	15 min	1 h	4 h	24 h
Blood	$3.18 \pm 0.91$	$1.22 \pm 0.62$	$0.76 \pm 0.46$	$0.90 \pm 0.48$
Heart	$3.36 \pm 1.06$	$2.05 \pm 1.45$	$1.63 \pm 0.73$	$2.69 \pm 1.09$
Lung	$5.19 \pm 1.76$	$2.96 \pm 1.84$	$3.27 \pm 1.31$	$3.55 \pm 1.17$
Liver	$14.97 \pm 3.37$	$9.56 \pm 5.20$	$8.98 \pm 2.74$	$7.80 \pm 1.51$
Stomach	$3.94 \pm 0.70$	$2.30 \pm 0.96$	$2.46 \pm 0.95$	$1.68 \pm 0.59$
Small intestines	$8.26 \pm 3.55$	$13.45 \pm 2.08$	$5.04 \pm 1.07$	$2.84 \pm 0.48$
Large intestines	$5.13 \pm 3.25$	$5.58 \pm 2.84$	$16.29 \pm 3.81$	$3.78 \pm 0.85$
Kidneys	$15.16 \pm 2.99$	$8.46 \pm 2.79$	$5.43 \pm 0.90$	$4.58 \pm 0.95$
Spleen	$2.68 \pm 1.60$	$2.52 \pm 1.59$	$3.57 \pm 2.23$	$3.59 \pm 2.48$
Pancreas	$23.30 \pm 4.43$	$13.81 \pm 2.69$	$12.16 \pm 1.34$	$3.65 \pm 0.44$
Muscle	$1.23 \pm 0.14$	$0.65 \pm 0.37$	$0.26 \pm 0.14$	$0.46 \pm 0.21$
Bone	$1.98 \pm 0.51$	$1.12 \pm 0.66$	$0.79 \pm 0.35$	$1.15 \pm 0.59$
Tumors	$4.95 \pm 0.91$	$3.48 \pm 0.90$	$3.00 \pm 1.10$	$3.88 \pm 1.40$
Excretion (%ID)	$19.13 \pm 6.94$	$44.63 \pm 9.15$	$49.77 \pm 8.19$	$67.84 \pm 5.43$

All data, except excretion, are presented as %ID/g  $\pm$  SD. Excretion data are presented as %ID  $\pm$  SD ( $n = 5$ ).

transchelation of the radiometal from the chelator to intracellular proteins (24,27,31).

In vivo pharmacokinetic studies show stark contrasts in the biodistribution and retention of  $^{64}\text{Cu}$ -DOTA-8-AOC-BBN(7–14) $\text{NH}_2$  and  $^{64}\text{Cu}$ -CB-TE2A-8-AOC-BBN(7–14) $\text{NH}_2$ . The blood retention of  $^{64}\text{Cu}$ -DOTA-8-AOC-BBN(7–14) $\text{NH}_2$  was  $1.22 \pm 0.62$  %ID/g at 1 h after injection, which on average declined slightly to  $0.90 \pm 0.48$  %ID/g at 24 h after injection. The significant blood retention is likely due to transchelation of the  $^{64}\text{Cu}$  radionuclide from the kinetically unstable DOTA chelation system to serum proteins such as serum albumin (25–27). The high blood activity associated with the  $^{64}\text{Cu}$ -DOTA-8-AOC-BBN(7–14) $\text{NH}_2$  conjugate results in abnormally high background activities in all tissues. In contrast, the  $^{64}\text{Cu}$ -CB-TE2A-8-AOC-BBN(7–14) $\text{NH}_2$  radioconjugate shows good blood clearance with  $0.51 \pm$

$0.14$  and  $0.05 \pm 0.03$  %ID/g at 1 and 24 h after injection, respectively. The significantly reduced blood retention of the  $^{64}\text{Cu}$ -CB-TE2A radioconjugate correlates with the enhanced kinetic stability offered by the CB-TE2A chelation system. The blood retention of the  $^{64}\text{Cu}$ -CB-TE2A bombesin radioconjugate is, to our knowledge, the lowest reported blood-associated activity at the 24-h time point after injection for a  $^{64}\text{Cu}$  bombesin analog to date.

In vivo unstable copper compounds are known to exhibit high retention in the liver. For the  $^{64}\text{Cu}$ -DOTA radioconjugate,  $7.80 \pm 1.51$  %ID/g remained in the liver at 24 h after injection. The  $^{64}\text{Cu}$ -CB-TE2A radioconjugate demonstrated significantly lower retention at 24 h after injection, with a liver-associated activity of  $0.21 \pm 0.06$  %ID/g. By RP-HPLC, the  $^{64}\text{Cu}$ -CB-TE2A radioconjugate was found to be more lipophilic than the  $^{64}\text{Cu}$ -DOTA radioconjugate.

**TABLE 3**  
In Vivo Pharmacokinetic Studies of  $^{64}\text{Cu}$ -CB-TE2A-8-AOC-BBN(7–14) $\text{NH}_2$  Using SCID Mice Bearing PC-3 Xenografts

Tissue/organ	15 min	1 h	4 h	24 h
Blood	$2.37 \pm 1.47$	$0.51 \pm 0.14$	$0.06 \pm 0.05$	$0.05 \pm 0.03$
Heart	$1.45 \pm 0.67$	$0.09 \pm 0.08$	$0.08 \pm 0.08$	$0.10 \pm 0.09$
Lung	$2.86 \pm 1.12$	$0.60 \pm 0.19$	$0.22 \pm 0.15$	$0.15 \pm 0.08$
Liver	$5.52 \pm 1.32$	$2.15 \pm 0.26$	$0.64 \pm 0.08$	$0.21 \pm 0.06$
Stomach	$2.56 \pm 0.62$	$0.94 \pm 0.27$	$1.65 \pm 2.63$	$0.05 \pm 0.04$
Small intestines	$12.88 \pm 2.06$	$13.17 \pm 1.21$	$1.78 \pm 0.57$	$0.11 \pm 0.04$
Large intestines	$4.27 \pm 0.97$	$3.52 \pm 1.12$	$17.70 \pm 7.06$	$0.20 \pm 0.08$
Kidneys	$21.66 \pm 8.58$	$5.26 \pm 0.58$	$1.88 \pm 0.53$	$0.28 \pm 0.22$
Spleen	$2.96 \pm 2.84$	$0.68 \pm 0.53$	$0.16 \pm 0.16$	$0.56 \pm 0.30$
Pancreas	$31.28 \pm 3.24$	$17.66 \pm 2.00$	$2.18 \pm 0.71$	$0.18 \pm 0.14$
Muscle	$0.88 \pm 0.38$	$0.26 \pm 0.15$	$0.10 \pm 0.07$	$0.22 \pm 0.17$
Bone	$2.15 \pm 2.01$	$0.58 \pm 0.41$	$0.39 \pm 0.25$	$0.29 \pm 0.10$
Tumors	$6.95 \pm 2.27$	$2.65 \pm 1.05$	$1.32 \pm 0.49$	$0.28 \pm 0.21$
Excretion (%ID)	$26.48 \pm 10.18$	$60.38 \pm 2.16$	$77.88 \pm 6.58$	$98.60 \pm 0.28$

All data, except excretion, are presented as %ID/g  $\pm$  SD. Excretion data are presented as %ID  $\pm$  SD ( $n = 5$ ).



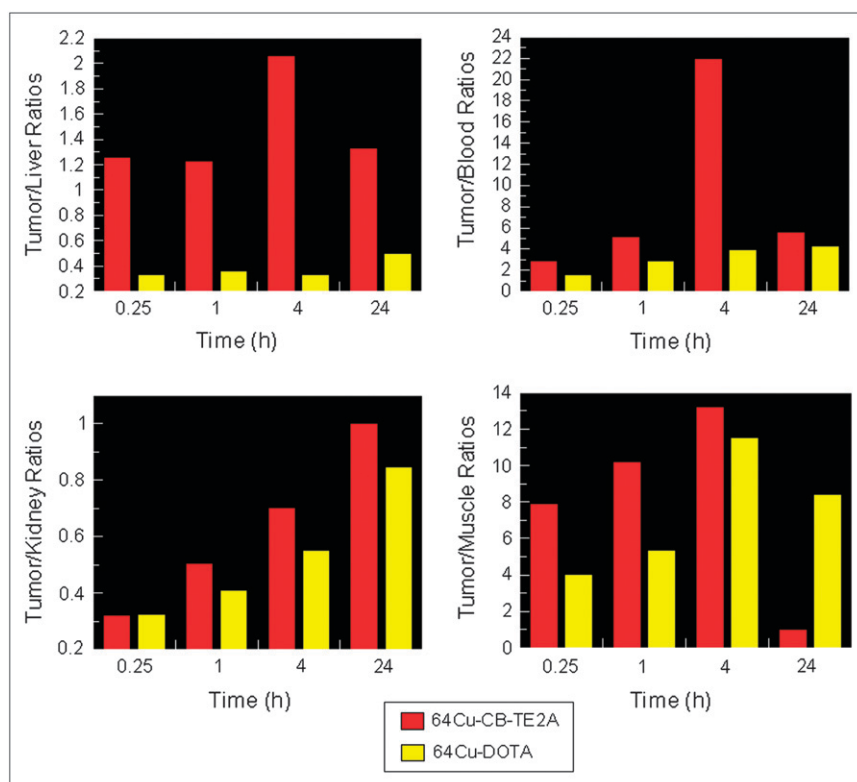


**FIGURE 5.** Comparison of  $^{64}\text{Cu}$ -CB-TE2A-8-AOC-BBN(7-14)NH<sub>2</sub> (red) and  $^{64}\text{Cu}$ -DOTA-8-AOC-BBN(7-14)NH<sub>2</sub> (yellow) using a radiolocalization index ([RI] %ID/g of tumor/%ID/g of nontarget tissue).

At 15 min after injection, the hepatobiliary clearance of the  $^{64}\text{Cu}$ -CB-TE2A-8-AOC-BBN(7-14)NH<sub>2</sub> radioconjugate ( $18.12 \pm 1.25$  %ID small intestines) was found to be significantly greater than the  $^{64}\text{Cu}$ -DOTA-8-AOC-BBN(7-14)NH<sub>2</sub> radioconjugate ( $9.58 \pm 3.95$  %ID small intestines). However, for  $^{64}\text{Cu}$ -DOTA-8-AOC-BBN(7-14)NH<sub>2</sub>, the considerable liver retention of  $^{64}\text{Cu}$ , likely due to transchelation, significantly reduces the amount of activity passed from the liver to the small intestines at the 15-min time point after injection.

Total excretion (urine and fecal) values for the 2 radioconjugates,  $^{64}\text{Cu}$ -CB-TE2A-8-AOC-BBN(7-14)NH<sub>2</sub> and  $^{64}\text{Cu}$ -DOTA-8-AOC-BBN(7-14)NH<sub>2</sub>, are in sharp contrast to one another. At 24 h after injection,  $98.60 \pm 0.28$  %ID of the  $^{64}\text{Cu}$  activity had been excreted (urine and feces) from the mouse using the  $^{64}\text{Cu}$ -CB-TE2A-8-AOC-BBN(7-14)NH<sub>2</sub> radioconjugate. The excretion values are consistent with those of the analogous radioconjugate,  $^{111}\text{In}$ -DOTA-8-AOC-BBN(7-14)NH<sub>2</sub> ( $87.2 \pm 4.3$  %ID excreted in urine at 24 h after injection). In contrast, only  $67.84 \pm 5.43$  %ID of the  $^{64}\text{Cu}$  activity was excreted from the mouse by 24 h after injection using  $^{64}\text{Cu}$ -DOTA-8-AOC-BBN(7-14)NH<sub>2</sub>. As the only difference between the 2 copper radioconjugates is the chelation system, the excretion values further support the hypothesis that the CB-TE2A conjugate substantially stabilizes the  $^{64}\text{Cu}$  radionuclide in vivo, thereby significantly reducing transchelation.

microPET/CT images of both radioconjugates at 20 h after injection (Fig. 6), using PC-3 tumor-bearing SCID

mice, agree well with the data obtained from pharmacokinetic studies. Because of biologic clearance properties of the radioconjugates, there was significantly less activity associated with the image of the  $^{64}\text{Cu}$ -CB-TE2A radioconjugate ( $\sim 370$  kBq [ $\sim 10$   $\mu\text{Ci}$ ]) compared with that of the  $^{64}\text{Cu}$ -DOTA radioconjugate ( $\sim 7.4$  MBq [ $\sim 200$   $\mu\text{Ci}$ ]). The PC-3 tumor xenografts in both mice are easily visualized in the normalized images and show similar tumor-to-background ratios. For the  $^{64}\text{Cu}$ -DOTA radioconjugate, the image revealed significant activity in the liver, kidneys, and gastrointestinal tract. The image using the  $^{64}\text{Cu}$ -CB-TE2A radioconjugate demonstrated considerably reduced activity located in the kidneys and gastrointestinal tract. Because of the markedly reduced activity in the liver using the  $^{64}\text{Cu}$ -CB-TE2A radioconjugate, the liver could not be easily visualized.

## CONCLUSION

The pharmacokinetic and microPET/CT studies demonstrate significantly improved nontarget tissue clearance properties associated with  $^{64}\text{Cu}$ -CB-TE2A-8-AOC-BBN(7-14)NH<sub>2</sub>. The significant improvement in clearance is attributed to the improved in vivo stability of the  $^{64}\text{Cu}$ -CB-TE2A chelate complex as compared with the  $^{64}\text{Cu}$ -DOTA chelate complex. While the stabilization of the  $^{64}\text{Cu}$  radionuclide using the CB-TE2A chelation system resulted in lower retention of the radiotracer in the PC-3 tumors, the substantial decrease in nontarget tissue retention significantly

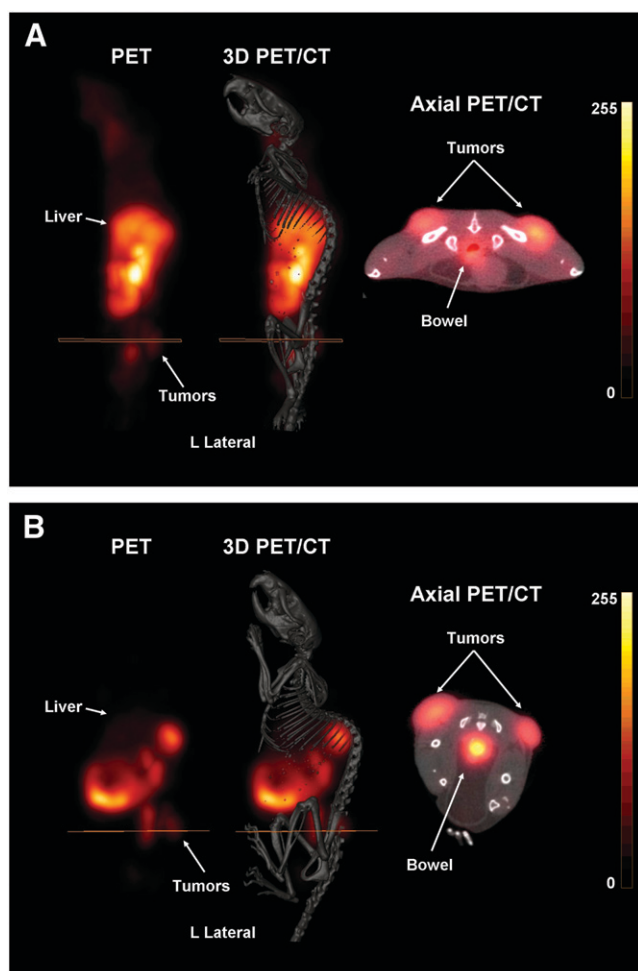


**FIGURE 6.** mircoPET, fused microPET/CT, and axial images of  $^{64}\text{Cu}$ -DOTA-8-AOC-BBN(7-14) $\text{NH}_2$  (A) and  $^{64}\text{Cu}$ -CB-TE2A-8-AOC-BBN(7-14) $\text{NH}_2$  (B) in PC-3 tumor-bearing SCID mice at 20 h after administration. Lateral and axial projection images have been normalized to the highest pixel intensity for each respective image.

increases the potential clinical applicability of  $^{64}\text{Cu}$  bombesin analogs for diagnostic imaging of prostate cancer. Future studies performed in our laboratory will focus on developing more hydrophilic  $^{64}\text{Cu}$  CB-TE2A bombesin analogs that exhibit higher renal clearance and increased tumor retention

## ACKNOWLEDGMENTS

The authors acknowledge Farah Naz, Nicholas R. Bell, Serena N. Carter, and Andrew Walters for useful discussions and their assistance with data collection and The Proteomics Center at the University of Missouri–Columbia for mass spectrometry services. This work was supported with the resources and the use of facilities at the Harry S. Truman Memorial VA Hospital. This work was also supported by grant NCI DHHS-R01-CA72942 from the National Cancer Institute, by grant ACS RSG-99-331-04-CDD

from the American Cancer Society, and by grant NIH DHHS-1P50-CA13013 from the National Institutes of Health. The University of Missouri holds U.S. patents 6 200 546, 6 921 526, 7 060 247, and 7 147 838 on technology described in this article, of which Timothy J. Hoffman, Gary L. Sieckman, and Wynn A. Volkert are coinventors.

## REFERENCES

- Smith CJ, Volkert WA, Hoffman TJ. Gastrin releasing peptide (GRP) receptor targeted radiopharmaceuticals: a concise update. *Nucl Med Biol.* 2003;30:861–868.
- Smith CJ, Volkert WA, Hoffman TJ. Radiolabeled peptide conjugates for targeting of the bombesin receptor superfamily subtypes. *Nucl Med Biol.* 2005;32:733–740.
- Zhou JH, Chen J, Mokotoff M, Ball ED. Targeting gastrin-releasing peptide receptors for cancer treatment. *Anticancer Drugs.* 2004;15:921–927.
- Anastasi A, Erspamer V, Bucci M. Isolation and amino acid sequences of alytesin and bombesin, two analogous active tetradecapeptides from the skin of European discoglossid frogs. *Arch Biochem Biophys.* 1972;148:443–446.
- Hoffman TJ, Gali H, Smith CJ, et al. Novel series of  $^{111}\text{In}$ -labeled bombesin analogs as potential radiopharmaceuticals for specific targeting of gastrin-releasing peptide receptors expressed on human prostate cancer cells. *J Nucl Med.* 2003;44:823–831.
- Akeson M, Sainz E, Mantey SA, Jensen RT, Battey JF. Identification of four amino acids in the gastrin-releasing peptide receptor that are required for high affinity agonist binding. *J Biol Chem.* 1997;272:17405–17409.
- Smith CJ, Gali H, Sieckman GL, et al. Radiochemical investigations of  $^{177}\text{Lu}$ -DOTA-8-Aoc-BBN[7-14] $\text{NH}_2$ : an in vitro/in vivo assessment of the targeting ability of this new radiopharmaceutical for PC-3 human prostate cancer cells. *Nucl Med Biol.* 2003;30:101–109.
- Smith CJ, Gali H, Sieckman GL, Higginbotham C, Volkert WA, Hoffman TJ. Radiochemical investigations of  $^{99\text{m}}\text{Tc}$ -N<sub>3</sub>S-X-BBN[7-14] $\text{NH}_2$ : an in vitro/in vivo structure-activity relationship study where X = 0-, 3-, 5-, 8-, and 11-carbon tethering moieties. *Bioconjug Chem.* 2003;14:93–102.
- Rogers BE, Bigott HM, McCarthy DW, et al. MicroPET imaging of a gastrin-releasing peptide receptor-positive tumor in a mouse model of human prostate cancer using a  $^{64}\text{Cu}$ -labeled bombesin analogue. *Bioconjug Chem.* 2003;14:756–763.
- Nock B, Nikolopoulou A, Chiotellis E, et al. [ $^{99\text{m}}\text{Tc}$ ]Demobesin 1, a novel potent bombesin analogue for GRP receptor-targeted tumour imaging. *Eur J Nucl Med Mol Imaging.* 2003;30:247–258.
- Lin K-S, Luu A, Baidoo KE, et al. A new high affinity technetium analogue of bombesin containing DTPA as a pharmacokinetic modifier. *Bioconjug Chem.* 2004;15:1416–1423.
- Lantry LE, Cappelletti E, Maddalena ME, et al.  $^{177}\text{Lu}$ -AMBA: synthesis and characterization of a selective  $^{177}\text{Lu}$ -labeled GRP-R agonist for systemic radiotherapy of prostate cancer. *J Nucl Med.* 2006;47:1144–1152.
- Chen X, Park R, Hou Y, et al. MicroPET and autoradiographic imaging of GRP receptor expression with  $^{64}\text{Cu}$ -DOTA-[Lys<sup>3</sup>]bombesin in human prostate adenocarcinoma xenografts. *J Nucl Med.* 2004;45:1390–1397.
- Van de Wiele C, Dumont F, Dierckx RA, et al. Biodistribution and dosimetry of  $^{99\text{m}}\text{Tc}$ -RP527, a gastrin-releasing peptide (GRP) agonist for the visualization of GRP receptor-expressing malignancies. *J Nucl Med.* 2001;42:1722–1727.
- Van de Wiele C, Dumont F, Vanden Broecke R, et al. Technetium-99m RP527, a GRP analogue for visualisation of GRP receptor-expressing malignancies: a feasibility study. *Eur J Nucl Med.* 2000;27:1694–1699.
- De Vincentis G, Remediani S, Varvarigou AD, et al. Role of  $^{99\text{m}}\text{Tc}$ -bombesin scan in diagnosis and staging of prostate cancer. *Cancer Biother Radiopharm.* 2004;19:81–84.
- Scopinaro F, De Vincentis G, Varvarigou AD, et al.  $^{99\text{m}}\text{Tc}$ -Bombesin detects prostate cancer and invasion of pelvic lymph nodes. *Eur J Nucl Med Mol Imaging.* 2003;30:1378–1382.
- Scopinaro F, Varvarigou AD, Ussof W, et al. Technetium labeled bombesin-like peptide: preliminary report on breast cancer uptake in patients. *Cancer Biother Radiopharm.* 2002;17:327–335.
- Bearn AG, Kunkel HG. Localization of  $\text{Cu}^{64}$  in serum fractions following oral administration: an alteration in Wilson's disease. *Proc Soc Exp Biol Med.* 1954;85:44–48.
- Thiers RE, Vallee BL. Distribution of metals in subcellular fractions of rat liver. *J Biol Chem.* 1957;226:911–920.

21. McCall JT, Davis GK. Effect of dietary protein and zinc on the absorption and liver deposition of radioactive and total copper. *J Nutr*. 1961;74:45–50.
22. Owen CA Jr, Hazelrig JB. Metabolism of  $^{64}\text{Cu}$ -labeled copper by the isolated rat liver. *Am J Physiol*. 1966;210:1059–1064.
23. Terao T, Owen CA Jr. Nature of copper compounds in liver supernate and bile of rats: studies with  $^{67}\text{Cu}$ . *Am J Physiol*. 1973;224:682–686.
24. Bass LA, Wang M, Welch MJ, Anderson CJ. In vivo transchelation of copper-64 from TETA-octreotide to superoxide dismutase in rat liver. *Bioconjug Chem*. 2000;11:527–532.
25. Moi MK, Meares CF, McCall MJ, Cole WC, DeNardo SJ. Copper chelates as probes of biological systems: stable copper complexes with a macrocyclic bifunctional chelating agent. *Anal Biochem*. 1985;148:249–253.
26. Cole WC, DeNardo SJ, Meares CF, et al. Serum stability of  $^{67}\text{Cu}$  chelates: comparison with  $^{111}\text{In}$  and  $^{57}\text{Co}$ . *Nucl Med Biol*. 1986;13:363–368.
27. Jones-Wilson TM, Deal KA, Anderson CJ, et al. The in vivo behavior of copper-64-labeled azamacrocyclic complexes. *Nucl Med Biol*. 1998;25:523–530.
28. Smith SV. Molecular imaging with copper-64. *J Inorg Biochem*. 2004;98:1874–1901.
29. Wong EH, Weisman GR, Hill DC, et al. Synthesis and characterization of cross-bridged cyclams and pendant-armed derivatives and structural studies of their copper(II) complexes. *J Am Chem Soc*. 2000;122:10561–10572.
30. Sun X, Wuest M, Weisman GR, et al. Radiolabeling and in vivo behavior of copper-64-labeled cross-bridged cyclam ligands. *J Med Chem*. 2002;45:469–477.
31. Boswell CA, Sun XK, Niu WJ, et al. Comparative in vivo stability of copper-64-labeled cross-bridged and conventional tetraazamacrocyclic complexes. *J Med Chem*. 2004;47:1465–1474.
32. Sprague JE, Peng YJ, Sun XK, et al. Preparation and biological evaluation of copper-64-labeled Tyr $^3$ -Octreotate using a cross-bridged macrocyclic chelator. *Clin Cancer Res*. 2004;10:8674–8682.
33. Woodin KS, Heroux KJ, Boswell CA, et al. Kinetic inertness and electrochemical behavior of copper(II) tetraazamacrocyclic complexes: possible implications for in vivo stability. *Eur J Inorg Chem*. 2005;4829–4833.
34. Parry JJ, Andrews R, Rogers BE. MicroPET imaging of breast cancer using radiolabeled bombesin analogs targeting the gastrin-releasing peptide receptor. *Breast Cancer Res Treat*. 2007;101:175–183.
35. Le Baccon M, Chuburu F, Toupet L, et al. Bis-animals: efficient tools for bis-macrocyclic synthesis. *New J Chem*. 2001;25:1168–1174.
36. Weisman GR, Wong EH, Hill DC, Rogers ME, Reed DP, Calabrese JC. Synthesis and transition-metal complexes of new cross-bridged tetraamine ligands. *Chem Commun*. 1996;947–948.
37. Taniuchi H, Fujibayashi Y, Okazawa H, Yonekura Y, Konishi J, Yokoyama A. Cu-pyruvaldehyde-bis( $\text{N}^4$ -methylthiosemicarbazone) (Cu-PTSM), a metal-complex with selective NADH-dependent reduction by complex-I in brain mitochondria: a potential radiopharmaceutical for mitochondria-functional imaging with positron emission tomography (PET). *Biol Pharm Bull*. 1995;18:1126–1129.
38. Hoffman TJ, Smith CJ, Gali H, et al.  $^{111}\text{In}/^{90}\text{Y}$  radiolabeled peptides for targeting prostate cancer: a matched pair gastrin releasing peptide (GRP) receptor localizing radiopharmaceutical [abstract]. *J Nucl Med*. 2001;42(suppl):274P–275P.
39. Rold TL, Garrison JC, Sieckman GL, et al. Targeting BB2 receptor expression in prostate cancer using promethium-149 labeled peptides. *97th Annual Meeting of the American Association for Cancer Research*. Washington, DC; April 1–5, 2006.



The Journal of  
NUCLEAR MEDICINE

## **In Vivo Evaluation and Small-Animal PET/CT of a Prostate Cancer Mouse Model Using $^{64}\text{Cu}$ Bombesin Analogs: Side-by-Side Comparison of the CB-TE2A and DOTA Chelation Systems**

Jered C. Garrison, Tammy L. Rold, Gary L. Sieckman, Said Daibes Figueroa, Wynn A. Volkert, Silvia S. Jurisson and Timothy J. Hoffman

*J Nucl Med.* 2007;48:1327-1337.

Published online: July 13, 2007.

Doi: 10.2967/jnumed.107.039487

---

This article and updated information are available at:

<http://jnm.snmjournals.org/content/48/8/1327>

---

Information about reproducing figures, tables, or other portions of this article can be found online at:


<http://jnm.snmjournals.org/site/misc/permission.xhtml>

Information about subscriptions to JNM can be found at:

<http://jnm.snmjournals.org/site/subscriptions/online.xhtml>

*The Journal of Nuclear Medicine* is published monthly.  
SNMMI | Society of Nuclear Medicine and Molecular Imaging  
1850 Samuel Morse Drive, Reston, VA 20190.  
(Print ISSN: 0161-5505, Online ISSN: 2159-662X)

© Copyright 2007 SNMMI; all rights reserved.

 SOCIETY OF  
NUCLEAR MEDICINE  
AND MOLECULAR IMAGING